Available online at www.sciencedirect.com
SCIENCE DIRECT®
Comparative Biochemistry and Physiology, Part B 142 (2005) 153 – 163
CBP
www.elsevier.com/locate/cbpb

Expression and tissue distribution of astacin-like squid metalloprotease (ALSM)

Nobuyuki Kanzawa*, Shuntaro Tatewaki, Ryousuke Watanabe, Ikuko Kunihisa, Haruka Iwahashi, Kaori Nakamura, Takahide Tsuchiya

Department of Chemistry, Faculty of Science and Technology, Sophia University, 102-8554, Tokyo, Japan

Received 28 January 2005; received in revised form 14 May 2005; accepted 15 May 2005
Available online 2 August 2005

Abstract

Astacin metalloprotease family members function in a wide variety of biologic events, including cell differentiation and morphogenesis during embryonic development and adult tissue differentiation. We previously isolated and characterized an astacin-like squid metalloprotease (ALSM). To elucidate the embryonic expression of ALSM, we performed immunohistochemical analysis with specific antibodies and examined the expression profiles of ALSM isoforms by in situ hybridization analysis. Tissue distribution and expression were also examined in adult spear squid. mRNA expression of ALSM isoforms I and III was first detected in newly hatched squid and was restricted to the liver. No mRNA signals were detected in other tissues even in adult squids. At the protein level, both isoforms were prominent in the liver of embryos and later in digestive organs of adult squid. Both isoforms were also detected in muscle tissues, including mantle and tentacle muscle. Staining for ALSM III was also identified in the iris and in tissues near the eye in squid embryos. However, no reactive bands were detected by immunoblotting of adult squid eyes. Thus, ALSM is initially expressed at the late stage of embryogenesis in spear squid, and expression is restricted to the liver. Thereafter, ALSM isoforms function in various tissues in an isoform-dependent manner.

Keywords: ALSM; Astacin; Embryo; Expression; Liver; Metalloprotease; Squid; Tissue distribution

1. Introduction

Astacin-like squid metalloprotease (ALSM) has a high substrate specificity for myosin heavy chain (MyHC) and was originally identified in squid mantle muscle (Okamoto et al., 1993; Tamori et al., 1999). Primary sequence analysis has shown that ALSM is a member of the astacin family (Yokozawa et al., 2002). Astacins were first identified as digestive enzymes (EC 3.4.24.21) in the stomach of the freshwater crayfish *Astacus astacus* (Titani et al., 1987; Dumermuth et al., 1991). Astacin family members have unique consensus sequences, including a zinc-binding sequence (HEXXHXXGFXHEXXRXDRD) and a Met-turn sequence (SXMHY) (Bode et al., 1993), and have been identified in various organisms from mammals to hydras (Bond and Beynon, 1995; Sarras, 1996). Studies of domain structure have revealed that astacins possess signal and prosequence domains along with a conserved protease domain characterized by the zinc-binding motif as well as a unique C-terminal domain specific to each family member. ALSM possesses signal, prosequence, and protease domains, followed by a MAM (meprin, A5 protein, receptor protein-tyrosine phosphatase μ) domain, which is a conserved domain in the C-terminus of meprin, an astacin family member (Bond and Beynon, 1995; Yokozawa et al., 2002). Astacins are involved in a wide variety of physiologic events, including digestion (Vogt et al., 1989), development (Takahara et al., 1994; Piccolo et al., 1996), hatching (Yasumasu et al., 1992a; Lee et al., 1994; Katagiri et al., 1997; Fan and Katagiri, 2001), regeneration (Yan et al., 2000a,b), and activation of hormones and some peptides (Yamaguchi et al., 1991). For example, human bone

* Corresponding author. Tel.: +81 3 3238 3363; fax: +81 3 3238 3361.
E-mail address: n-kanza@sophia.ac.jp (N. Kanzawa).

1096-4959/$ - see front matter © 2005 Elsevier Inc. All rights reserved.
doi:10.1016/j.cbpc.2005.05.018

morphogenetic protein 1 (huBMP1) induces ectopic bone formation in adult vertebrates (Wozney et al., 1988); *Drosophila* tolloid is required for normal dorsal patterning (Shimell et al., 1991; Marques et al., 1997); and meprins are found in mammalian kidney and intestinal tissues and play crucial roles in the processing of biologically active peptides and extracellular matrix (ECM) proteins (Craig et al., 1987; Bond and Beynon, 1995). An astacin-like protein from the freshwater polyp *Hydra vulgaris*, described as hydra metalloprotease I (HMP-1), is localized in the ECM in a head-specific manner and has a functional role during development (Yan et al., 1995). The fish hatching enzymes, high and low choriolytic enzymes (HCE/LCE), are secreted from hatching glands and digest the egg envelope (Yasumasu et al., 1992b; Inohaya et al., 1995). Thus, astacins have unique functions in each tissue in which they are expressed. ALSM can hydrolyze MyHC; therefore, it is thought to be involved in the metabolism of skeletal muscle proteins (Okamoto et al., 1993). Tissue distribution analysis of ALSM activity with the use of MyHC as an in vitro substrate revealed that ALSM exists in a wide variety of tissues, particularly in digestive organs (Tajima et al., 1998; Tamori et al., 1999). Two groups of ALSM isoforms are present in squid: types I and III in spear squid and types I and II in Japanese common squid. These isoforms are classified according to specificity for hydrolytic sites in rabbit skeletal muscle MyHC. Differentially regulated expression and distribution of the two groups of astacins have been reported in hydra (Yan et al., 2000a,b). However, the exact expression profiles of astacin isoforms have not been reported.

In the present study, we obtained specific antibodies for ALSM I and III isolated from spear squid (*Loligo bleekeri*) and examined the tissue distributions of ALSM isoforms in squid by immunohistochemistry. Expression of ALSM mRNA in the squid was examined by in situ hybridization and northern blotting and RT-PCR analysis.

2. Materials and methods

2.1. Materials

Spear squid (*Loligo bleekeri*) were purchased from the Tokyo Central Wholesale Fish Market. Spear squid eggs and embryos were a kind gift from Dr. Yuzuru Ikeda, Ryukyu University, and were fixed immediately in 4% paraformaldehyde for histochemical and immunohistochemical analyses or frozen in liquid nitrogen for biochemical analysis. Embryos were collected from eggs incubated in a small aquarium after approximately 6, 8, and 10 weeks of incubation. Eggs incubated for 6 or 8 weeks were extracted from the egg capsules, and the embryos were removed from the eggs. Embryos after 10 weeks of incubation were at the hatching stage. Embryos were inspected under light microscopy (Fig. 1), and embryonic stages were determined on the basis of morphologic characteristics according to the criteria of Baeg et al. (1992). Embryos after 6 weeks of incubation had large yolk sacs compared to the embryonic body; red retinas and red chromatophores were evident on the mantle surface but not on the tentacles, as is typical of stage 23 of embryonic development. In embryos after 8 weeks of incubation, the yolk sac and head were approximately the same size, which is typical of stage 26. Another marker of this stage, a filled ink sac, was also visible through the mantle muscle. Newly hatched embryos were classified as stage 28 embryos.

2.2. Expression of recombinant proteins

Recombinant ALSM I and III of spear squid were expressed in *Escherichia coli* for antibody specificity tests. ALSM I and III cDNAs were amplified from isolated clones (Yokozawa et al., 2002) by PCR with primer pairs (summarized in Table 1) of Y1-20 and T3 primer, and Y3-1 and Y3-2, respectively. Amplified fragments were

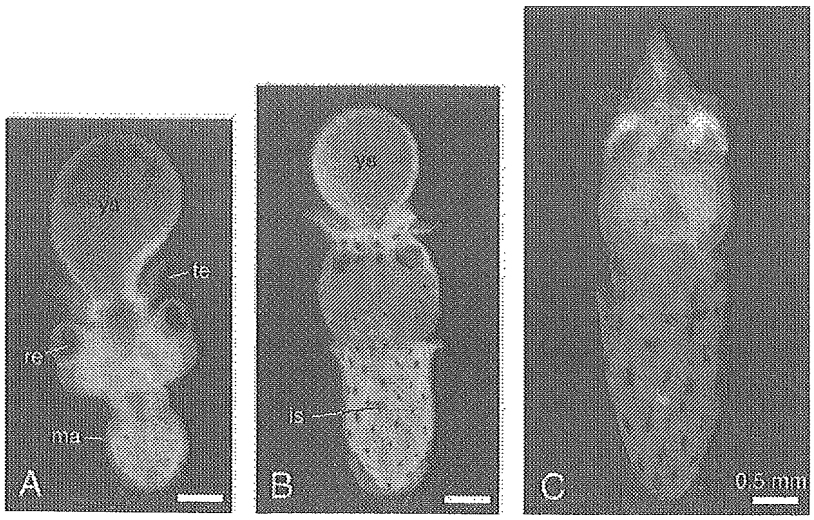

Fig. 1. Light micrographs of spear squid embryos at stages 23 (A), 26 (B), and 28 (C) is, ink sac; ma, mantle; re, retina; te, tentacle; ys, yolk sac.

Table 1
Oligonucleotide primers used for PCR amplification

Target gene	Primer name	Direction	Sequence
Spear squid (Loligo bleekeri)			
ALSM I	Y1-20	forward:	5′-CCATGGCTGTACCTCTGGACACCGAGC-3′
	Y1-15	reverse:	5′-CCGGATCCTTAACATTTTCCATC-3′
ALSM I	Y1-7	forward:	5′-GGGCATATGCTGGGTGGTGGATGTCGTG-3′
	Y1-12	reverse:	5′-GAATTCTCATGAATTGTAATCGTA-3′
ALSM III	Y3-1	forward:	5′-GGATCCATGGCAAACGCAATTGGTAATCTCAAA-3′
	Y3-2	reverse:	5′-GGATCCATGGCACAACTTCCAGGTGTAAGTAAA-3′
ALSM III	Y3-h	forward:	5′-GGTCTTCCATATGATTACAATTC-3′
	Y3-t	reverse:	5′-TCATCTGTTTCCATTTATTTCCTT-3′
actin	Actin-f	forward:	5′-TCTGGCACCACACCTTCTACA-3′
	Actin-r	reverse:	5′-GCCACGTAGCACAGCTTCTC-3′
Japanese common squid (Todarodes pacificus)			
ALSM I	S1-1	forward:	5′-GGATCCATGGCAAGTGTTGTTGGAGATCTTAAC-3′
	S1-2	reverse:	5′-GGATCCATGGCGCATCTTCCATCCAGAATAAA-3′
ALSM II	S2-1	forward:	5′-GGATCCATGGCAAACGCAGTTGGTAGCATCAAA-3′
	S2-2	reverse:	5′-GGATCCATGGCACATTT CCCAGGCGTAAGTACG-3′

then ligated into the pGEM-T Easy Vector (Promega, Madison, WI, USA). An insert of ALSM I containing sequence for the propeptide, protease, and MAM domains was digested with *Nco*I/*Eco*RI and further ligated into the expression vector pET32b (Novagen, Madison WI, USA) to express a thioredoxin-fused protein (65 kDa). An insert of ALSM III containing the protease and MAM domains was digested with *Nco*I enzyme and ligated into the *Nco*I site of the expression vector pETGEX-CT (Sharrocks, 1994) provided from the Department of Microbial Genetics, National Institute of Genetics (Shizuoka, Japan), and the direction was determined by sequencing of isolated clones. *E. coli* (BL21) were transformed with isolated clones, and expression of glutathione-*S*-transferase (GST)-fused protein (62 kDa) was induced by 1 mM IPTG.

Recombinant ALSM I and II from Japanese common squid (*Todarodes pacificus*) were also expressed in *E. coli* for use in antibody specificity tests. ALSM I and II were amplified with primer pairs of S1-1 and S1-2, and S2-1 and S2-2, respectively. Both amplified fragments were ligated into the pGEM-T Easy Vector and then subclone into the pETGEX-CT expression vector. Ligation and transformation of *E. coli* were performed by the same technique as that for spear squid ALSM III. The relative molecular masses of GST-fused proteins of Japanese common squid ALSM I and II were 62 kDa and 65 kDa, respectively.

2.3. Antibody generation and immunoblot analysis

The polyclonal antibody (TY-ID) generated against a small peptide from spear squid ALSM I was characterized previously (Yokozawa et al., 2002). To generate an antibody against spear squid ALSM III, GST-fused ALSM III was expressed in *E. coli* as described above, purified on glutathione-agarose beads according to the manufacturer's instructions (Amersham Pharmacia Biotech, Little Chalfont, UK), and cleaved with 1 unit/L thrombin (Sigma-Aldrich Chemical Co., St. Louis, MO, USA). Cleaved ALSM III with protease and MAM domains was resolved by sodium dodecyl sulfate polyacrylamide gel electrophoresis (SDS-PAGE) (Laemmli, 1970) followed by electrophoretic elution of ALSM III peptide from the gels. The purified peptide was dialyzed against phosphate-buffered saline (PBS) and used as antigen. Rabbits were immunized with the antigen emulsified in Freund's complete adjuvant and were boosted twice with the same antigen emulsified in Freund's incomplete adjuvant. Serum containing anti-ALSM III antibody was purified by incubating the serum with nitrocellulose-bound antigen and then eluting it at low pH (Sambrook et al., 1989). Purified antibody to ALSM III was designated as KY-III.

To confirm the specificity of the generated antibodies, crude liver extracts of adult spear squid were incubated with antibody and protein A-Sepharose (Amersham Pharmacia Biotech). Immune complex was washed three times with PBS and divided into the half. One was eluted by the SDS-sample solution (10% glycerol, 10% 2-mercaptoethanol, 3% SDS, and 62.5 mM Tris–HCl, pH 6.7) and then was resolved by 12% SDS-PAGE. The other half was incubated with rabbit skeletal muscle myosin to examine the enzyme activity (Tamori et al., 1999). Briefly, immune complex was mixed with reaction mixture to give final concentrations of 0.6 mg/mL rabbit skeletal muscle myosin, 100 mM sodium phosphate, pH 7.2, 5 mM EDTA, 4 mM MIA, 8 mM phenylmethylsulphonyl fluoride (PMSF), 20 μg/mL pepstatin A, 20 μg/mL leupeptin, and 10 mM $ZnCl_2$. After incubation for overnight at 37 °C, the reaction was stopped by addition of SDS sample solution. Aliquots of the sample were subjected to 10% SDS-PAGE.

2.4. Tissue sectioning and immunohistochemistry

Spear squid embryos fixed in paraformaldehyde were rinsed with PBS several times and frozen in Tissue-Tek

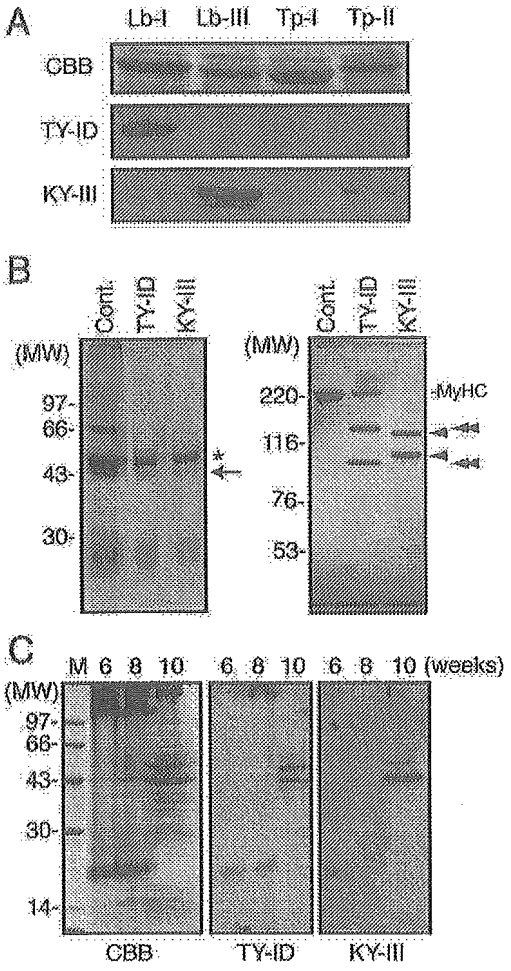

Fig. 2. Specificity tests of antibodies against ALSM isoforms. A, Lb-I and Lb-III, *Loligo bleekeri* ALSM I and III. Tp-I and Tp-II, *Todarodes pacificus* ALSM I and II. Bacterially expressed isoforms were subjected to SDS-PAGE and either stained with Coomassie Brilliant Blue (CBB) (top panel) or detected with antibodies to ALSM I (TY-ID) or III (KY-III). B, Crude liver extracts of adult spear squid were incubated with pre-immune serum (Cont.), TY-ID and KY-III, and precipitated with protein A-Sepharose. Precipitates were eluted and resolved by SDS-PAGE (left panel). Asterisk shows the major band of antibody heavy chain. Arrow represents the molecular size of ALSMs. Enzyme activity was examined with the precipitates (right panel). No hydrolysis of rabbit skeletal muscle heavy chain (MyHC) was observed in control; however, 130 and 90 kDa fragments (arrowheads), and 120 and 100 kDa fragments (double-arrowheads) were observed when rabbit myosin was incubated with immunoprecipitate with TY-ID and KY-III, respectively. C, Immunoblot analysis of ALSM isoforms in spear squid embryos incubated 6 (stage 23), 8 (stage 26), and 10 (stage 28) weeks. Approximately 10 μg of total protein from each sample extract was subjected to SDS-PAGE followed by staining with CBB or detection with antibodies to ALSM isoforms. Both ALSM I (TY-ID) and III (KY-III) were detected in extracts of stage 28 embryos as a doublet. No signals were detected at other embryonic stages.

OCT compound (Miles, Elkhart, IN, USA) or mounted in low-melt wax as follows: Embryos were dehydrated in a graded ethanol/PBS series (30%, 50%, 70%, 90%, and 100% ethanol), 1 h per step at 4 °C. After two incubations in 100% ethanol, the specimens were stored at 4 °C overnight. Embedding was carried out at 37 °C, first for 30 min in 100% ethanol at 37 °C, then in a graded 100% ethanol/low-melt wax (Steedman, 1957) series (2:1, 1:1, 1:2 *v/v*) followed by three changes of pure wax, each for 1–2 h, and overnight incubation at 37 °C. Specimens were then placed into embedding molds and left to polymerize overnight at room temperature. Ribbons of 10-μm sections were placed on albumin-coated slides and stretched by the addition of a small drop of distilled water to one end of the ribbon. For dewaxing and rehydration of sections, specimens were immersed in an ethanol/PBS series (100%, 70%, 50%, 30%, and 10% ethanol), 10 min per step at room temperature. After two incubations in PBS for 10 min each, the specimens were used for histochemical or immunohistochemical analysis.

Indirect immunofluorescence was performed as described previously (Yokozawa et al., 2002). Briefly, specimens were permeabilized at room temperature in 0.1% Triton X-100 for 5 min. After a washing with PBS, nonspecific binding was blocked with 10% normal goat serum and 3% bovine serum albumin (BSA) in PBS for 1 h. Double immunolabeling was performed with anti-actin antibody (diluted 1:2000, clone C4; ICN Pharmaceuticals Inc., Costa Mesa, CA, USA) and affinity purified polyclonal antibodies TY-ID or KY-III (diluted 1:100). The secondary antibodies were Alexa 594-conjugated goat anti-mouse IgG_1 antibody (diluted 1:150; Molecular Probes, Eugene, OR, USA) for the C4 antibody and fluorescein-labeled goat anti-rabbit IgG antibody (Kirkegaard and Perry Laboratories Inc., Gaithersburg, MD, USA) for the TY-ID and KY-III antibodies. Specimens were examined with a confocal microscope (LSM410; Carl Zeiss Inc., Oberkochen, Germany).

2.5. Analysis of ALSM III mRNA expression in embryonic tissue sections

To obtain sense and antisense riboprobes for ALSM I, a small fragment (250 bp) was PCR amplified with the primer pair of Y1-7 and Y1-12, and ligated into the pGEM-T Easy Vector. The obtained subclone was linearized and used as a template for the generation of riboprobes with a MAXIscript In Vitro Transcription Kit (Ambion Inc., Austin, TX, USA). Specificity of the probe was tested against clones of ALSM I and III (data not shown). In situ hybridization (Henrique et al., 1995) was performed as described previously (Takebayashi-Suzuki et al., 2000; Kanzawa et al., 2002). Briefly, sections prepared as described above were treated with 20 μg/mL proteinase K for 3 min at room temperature. After post-fixation with 4% paraformaldehyde in PBS for 10 min at room temperature, specimens were rinsed with PBS, preincubated with the hybridization mixture for 30 min at 65 °C, and reacted overnight at 65 °C with 0.5–1.0 μg/mL digoxigenin (DIG)-labeled riboprobe. After 60 °C washes and blocking, the samples were incubated overnight at 4 °C with alkaline phosphatase-conjugated anti-DIG antibody (diluted 1:2000, Roche, Switzerland). After washing to remove unbound antibody, samples were stained with NBT/BCIP mixture at room temperature for color development.

2.6. Northern blotting and RT-PCR analysis

Total RNA was extracted with TRIzol reagent (Invitrogen), and approximately 30 μg of total RNA was separated on a 1.0% agarose/formaldehyde gels and transferred to a Hybond-N+ membrane (Amersham). Probes for Northern hybridization were prepared as follows: Partial sequences were amplified from isolated clones by PCR with primer pairs of Y1-7 and Y1-12 for ALSM I, and Y3-h and Y3-t for ALSM III, and amplified fragments were ligated into pGEM-T Easy Vector. Insert digested with *Eco*RI was used as specific probe. Probe labeling, hybridization and detection were performed with the ECL Direct Nucleic Acid Labelling and Detection System (Amersham) according to the manufacturer's instructions.

RT-PCR was performed with total RNA as follows: After reverse transcription with oligo-dT primer, DNA was amplified using primers against each specific sequence; Y1-20 and Y1-15 for ALSM I, Y3-1 and Y3-2 for ALSM III, and actin-f and actin-r for actin. PCR reaction conditions for ALSM I and actin included initial denaturation for 2 min at 95 °C followed by 30 cycles at 95 °C for 45 s, 56 °C for 45 s, and 72 °C for 90 s each plus a final incubation for 3 min at 72 °C. PCR amplification for ALSM III was performed as described above except the annealing temperature was 58 °C. Yielded products of ALSM I, III, and actin were 1261bp, 1142 bp, and 406 bp, respectively. PCR products were resolved on 1% agarose gels and stained with 1 μg/mL ethidium bromide.

3. Results

3.1. Antibody specificity

To generate a specific antibody against ALSM III, recombinant protein containing the propeptide, protease, and MAM domains was used to immunize rabbits, and antibody was purified from the serum and designated as KY-III. To characterize the antibody specificity, immunoreactivity to bacterially expressed ALSMs was examined (Fig. 2A). TY-ID recognized ALSM I from spear squid (Lb-I) but not isoform from Japanese common squid (Tp-1). This is due to the difference in peptide sequence, which was used to generate TY-ID (Yokozawa et al., 2002). KY-III recognized ALSM III from spear squid (Lb-III) and, to a lesser extent, ALSM II from Japanese common squid (Tp-II). To certificate the specificity of antibodies, we performed immunoprecipitation experiments with the generated antibodies. The band of ALSM isoforms precipitated with antibodies was not confirmed clearly, because of the presence of antibody heavy chain at the similar molecular masses (Fig. 2B, left panel). However, precipitates exhibited specific activities to hydrolyze myosin heavy chain (Fig.

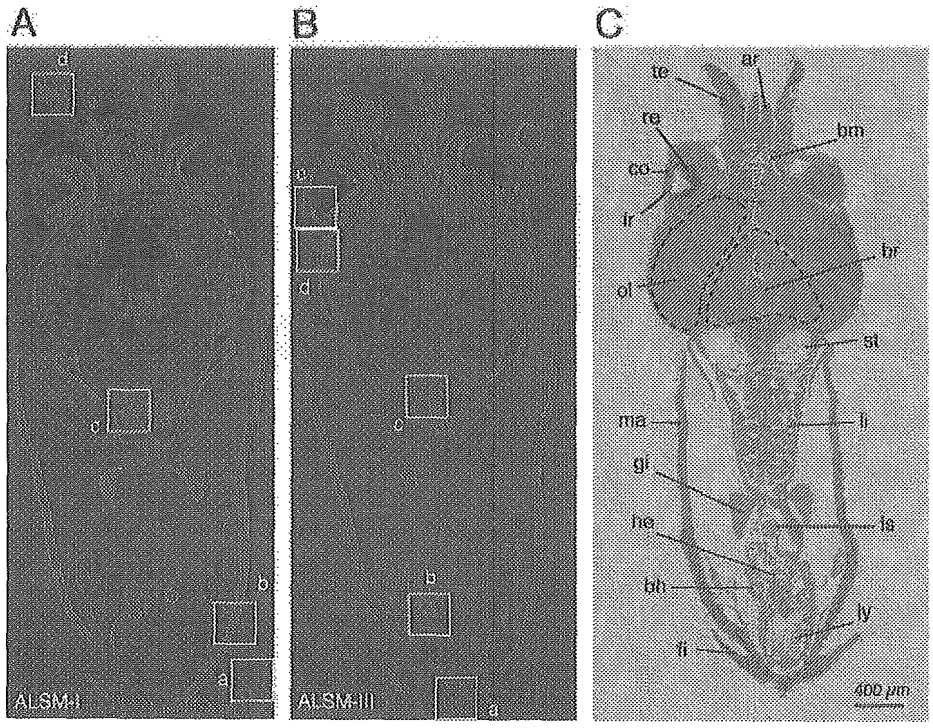

Fig. 3. Overview of the immunohistochemical distribution of ALSM isoforms in newly hatched squid (stage 28). Merged images were obtained by double immunostaining with specific antibodies against cellular actin (red) and ALSM isoforms (green), ALSM I (A), or III (B). White boxes (a–d in panel A and a–e in panel B) correspond to the panel numbers in Figs. 4 and 5, respectively. C, Light micrograph of a section of newly hatched squid (stage 28). ar, arm; bh, branchial heart; bm, buccal mass; br, brain; co, cornea; fi, fin; gi, gill; he, heart; is, ink sac; ir, iris; iy, inner yolk; li, liver; ma, mantle; ol, optic lobe; re, retina; st, statocyst; te, tentacle.

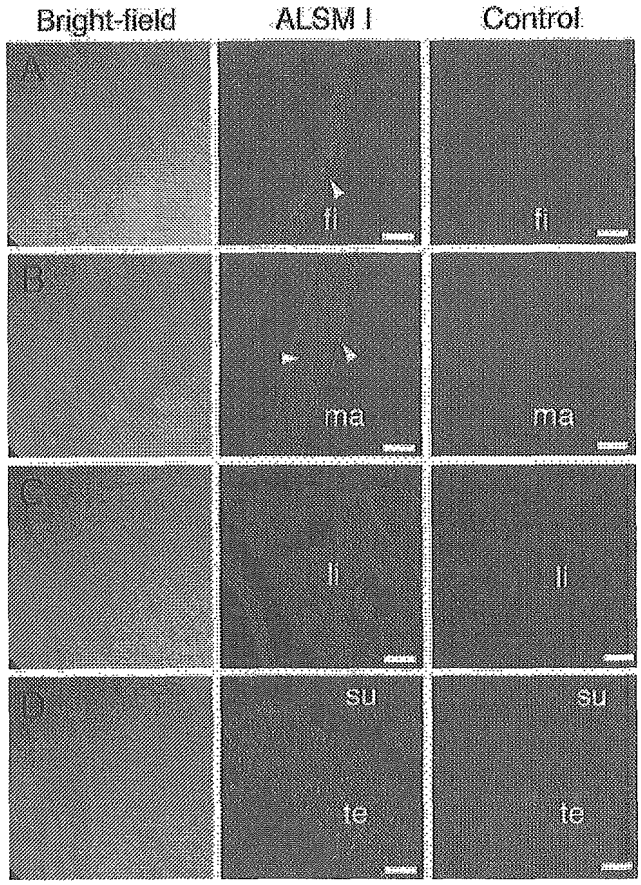

Fig. 4. Higher-magnification images of the tissue distribution of ALSM I. Merged images shows the distribution of cellular actin (red) and ALSM isoforms (green). Immunofluorescence analysis detected ALSM I staining in muscle tissues, including (A) lateral fin (fi), (B) mantle (ma), and (D) tentacle (te). Strong staining was also detected in (C) the liver (li). (Control), Negative control in the absence of primary antibody. su, sucker. Bars indicate 50 μm.

2B, right panel). Immunoblot analysis of tissue extracts showed a doublet at stage 28 (10 weeks), with a major 45-kDa band and a minor 50-kDa band (Fig. 2C). Thus, we concluded that the antibodies specifically recognized each isoform.

3.2. Tissue distributions of ALSM isoforms in embryos

We examined the embryonic tissue distribution of ALSM isoforms by indirect immunofluorescence analysis. ALSM is a secreted protein reportedly localized in the extracellular region of the mantle muscle (Yokozawa et al., 2002). Distribution in other tissues has not been reported. To determine the extracellular localization, we performed double immunostaining with the ALSM antibodies and an actin antibody, which recognizes cytoplasmic actin (Fig. 3). With both ALSM antibodies, a strong green signal was identified in the retina. However, a similar signal was seen in the absence of primary antibody as described below, suggesting that the signal in the retina was due to autofluorescence. Staining for ALSM I was detected in muscle tissues, including mantle, fin, and tentacles. In contrast, no obvious staining for ALSM III was detected in muscle tissues except fin. Both ALSM I and III staining was detected in the fin. ALSM I staining was distributed over the fin (Fig. 4a), whereas ALSM III staining in the fin was confined to the central area (Fig. 5a). Staining for ALSM I and III was detected in the liver (Figs. 4c and 5c) and the membranous tissue surrounding the inner yolk (Fig. 5b). Interestingly, staining for ALSM IIII was obvious in the iris (Fig. 5e) and in tissue connected to the cornea (Fig. 5d). However, no staining for ALSM I was detected in these regions.

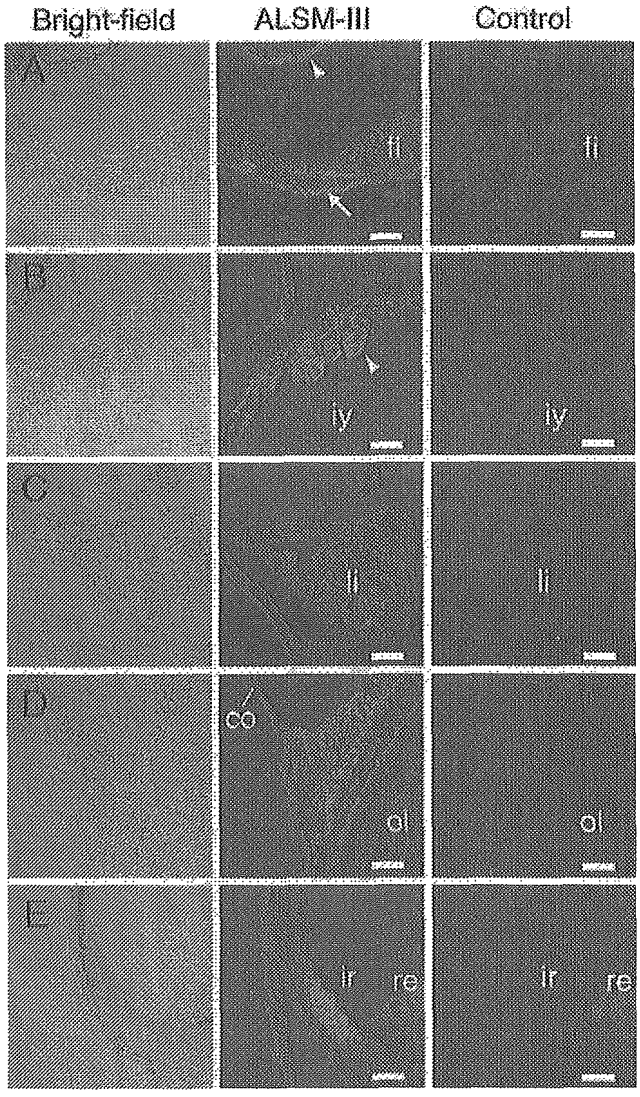

Fig. 5. Higher-magnification images of tissue distribution of ALSM III. Merged images shows the distribution of cellular actin (red) and ALSM isoforms (green). Immunofluorescence analysis detected ALSM III in (A) center area of the fin (fi) as indicated by arrow and in membranous tissue surrounding the inner yolk (iy) as indicated by arrowheads in (A) and (B). Strong staining was detected in (C) the liver (li) compared to the negative control in the absence of primary antibody. ALSM III staining was also detected in (D) tissue connected to the cornea (co) and in (E) the iris (ir). ol, optic lobe. (re) represents the non-specific autofluorescence detected in retina. Bars indicate 50 μm.

We reported that immunoblot analysis showed ALSM I to be distributed in a wide variety of tissues in adult spear squid (Yokozawa et al., 2002). However, expression of ALSM mRNA has not been reported. In situ hybridization analysis of stage 28 embryos showed expression of ALSM I mRNA to be confined to the liver (Fig. 6B and D). However nonspecific sense signals were present in the lower tip of the body and in the ink sac, retina, and cornea (Fig. 6A). In the optic lobe, signals detected with the anti-sense probe were stronger than those detected with the sense probe. However, this may also have been nonspecific background. Nonspecific signals were also detected at the lower tip of the body and in the retina in stage 26 embryos, and no obvious differences were identified between sense and anti-sense probes at this stage (Fig. 6E and F).

3.3. Tissue distributions and expression of ALSM isoforms in adult squid

To examine the expression levels of ALSM isoforms in adult squid, specific probes for northern blot analysis were prepared by PCR amplification. Probes for ALSM I and III were 68% and 58% identical to the corresponding sequences of each isoform. Probe specificity was further confirmed by Southern blot analysis against isolated cDNA clones (data not shown). With northern blotting, each isoform was detected below the ribosomal RNA (approximately 2 kb), and the staining was detected only for the liver (Fig 7A). Consistent with biochemical findings (Tamori et al., 1999; Yokozawa et al., 2002), signals for ALSM III were stronger than signals for ALSM I. Restricted expression was further analyzed by RT-PCR (Fig. 7B). Approximately 30 ng of complementary DNAs for each isoform was used as template. Actin as an internal control was detected in all tissues. Amplified fragments for each isoform were detected only in the liver. Thus, expression of ALSM isoforms seems to be restricted to the liver of adult squid.

We reported previously that ALSM I was widely distributed in tissues (Yokozawa et al., 2002). In this study, we examined tissue distribution of ALSM III. An immunoreactive band was detected at 45 kDa; staining was prominent for digestive organs, including stomach, liver, and pancreas and week in muscle tissues such as branchial heart, mantle, and tentacle (Fig. 8); a 30-kDa degradation product of ALSM was mainly detected in the mantle. In embryos, staining of ALSM III was present in the iris and in tissue connected to the cornea. However, no immunoreactive bands were detected by immunoblotting of adult squid eyes. Distribution of ALSM III was further examined by double immunostaining with anti-actin antibody. Patchily staining of ALSM III was detected (Fig 9B) and distributed extracellularly in the mantle muscle (Fig. 9C), unlike the intracellular distribution of actin (Fig. 9A). Squid liver consists of hepatic lobules, as indicated by the dashed-line in Fig. 9D. Staining of actin was detected in the boundary area of the lobules (double arrowhead in Fig. 9E) and periphery of the central vein (arrowheads in Fig. 9E). Strong staining of ALSM III was detected in hepatic cells, and

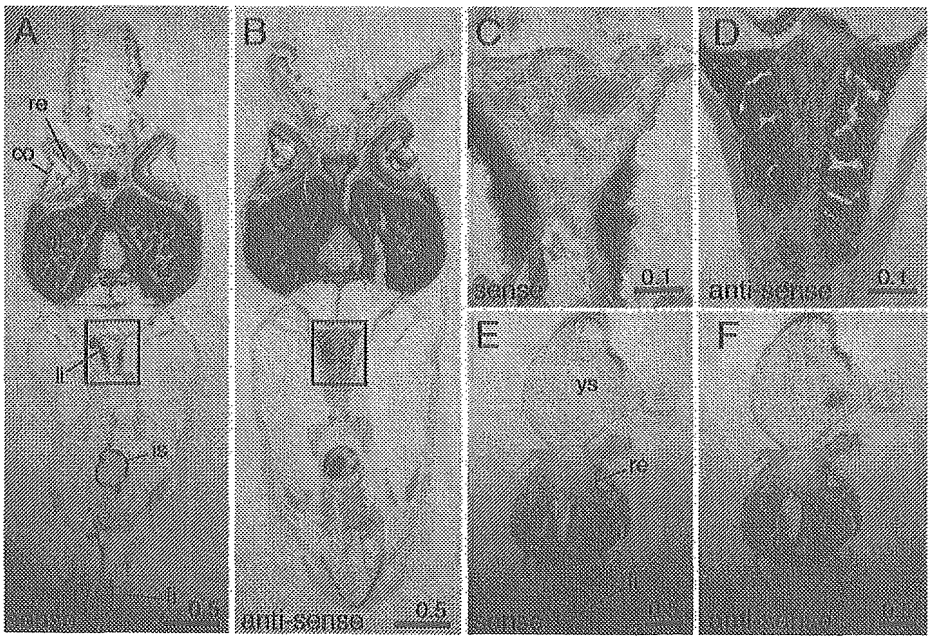

Fig. 6. In situ hybridization. Sections (16-μm thickness) were prepared from frozen squid embryos at stage 28 (A, B, C, and D) and 26 (E and F). Sense and anti-sense riboprobes were used to detect specific signal for ALSM I mRNA. (C and D), High-power views of boxed areas in A and B show expression of ALSM I mRNA in the liver (li). Non-specific sense signals were seen in lower tip of body near the fin (fi), ink sac (is), retina (re), and cornea (co) at stage 28 embryo. Bars in A, B, E, and F are 0.5 mm; bars in C and D are 0.1 mm. ys, yolk sac.

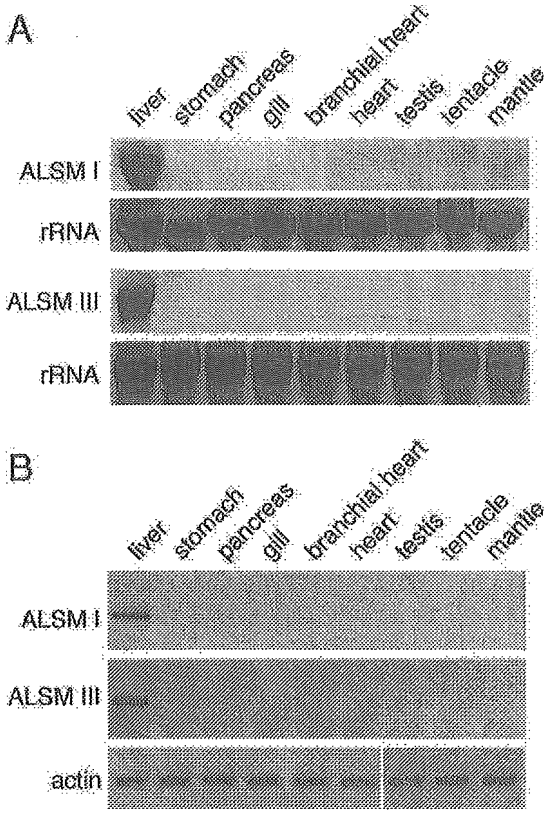

Fig. 7. mRNA expression of ALSMs in adult squid. (A) Northern blot analysis of ALSM isoforms in tissues of adult spear squid. Approximately 30 μg of total RNA was separated on 1% agarose/formaldehyde gels, stained with ethidium bromide (lower panes), and hybridized with specific probes (ALSM I and ALSMIII in upper panes). rRNA, ribosomal RNA. (B) RT-PCR analysis of ALSM isoforms in tissues of adult spear squid. Complementary DNAs (cDNAs) were reverse-transcribed from total RNAs with oligo-dT primer. Approximately 30 ng of cDNA was used as template in the PCR reaction under the conditions described in the Materials and methods.

weak staining was detected in interlobular artery or interlobular vein (Fig. 9F).

4. Discussion

Astacins are widely distributed in vertebrates and invertebrates. Recent analysis has shown that astacins are associated with a wide range of physiologic events and that some astacins are multifunctional proteases (Bond and Beynon, 1995; Sarras, 1996). The genome-sequencing of *Caenorhabditis elegans* identified 40 genes that code for astacin-like proteins, and they are classified into six groups by comparison of the highly conserved protease domain and unique C-terminal domain. Their expression levels and profiles are highly organized developmentally (Mohrlen et al., 2003). One astacin group with conserved protease and MAM domains has been identified in squid. Two isoforms, ALSM I and II for Japanese common squid and ALSM I and III for spear squid have been cloned and characterized. ALSM was originally identified as a metalloprotease, which hydrolyzes MyHC specifically, and was thought to be involved in muscle metabolism (Okamoto et al., 1993). However, our recent analysis has shown that ALSM is a secreted protease. To elucidate the physiologic roles of ALSM in vivo, we examined embryonic expression and distribution of ALSM isoforms. Tracking squid throughout their lives can be difficult, and handling and feeding techniques for spear squid are not well established. Survival after hatching in small aquariums is quite low (Y. Ikeda, personal communication). In the present study, we obtained squid embryos at three stages of development. To determine ALSM tissue distributions, we used specific antibodies for ALSM I (TY-ID, (Yokozawa et al., 2002)) and III (KY-III). These antibodies are specific to each isoform, as shown in Fig. 2. However, bands detected in extracts from stage 28 embryos were seen as doublets, indicating that the antibodies recognize not only the mature protein (45 kDa) but also the precursor peptide (50 kDa) of each isoform. With the same antibodies, only a single band (45 kDa) was detected in tissue extracts from adult spear squid (Fig. 8B), suggesting the presence of a mechanism controlling the differentiation of precursor ALSM to mature ALSM. The physiological roles of astacins in development have been well studied in fish. HCE and LCE of medaka are choriolytic enzymes secreted from unicellular hatching glands to digest the egg envelope. Expression of HCE and LCE is detected in the late gastrula until just before hatching (Inohaya et al., 1995; Hiroi et al., 2004). Immunoblot analysis revealed that ALSM isoforms are expressed in

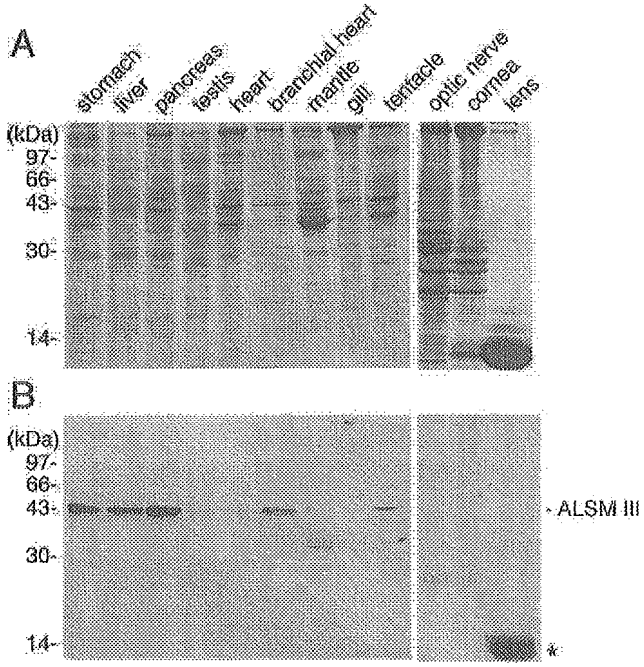

Fig. 8. Tissue distribution of ALSM III in adult spear squid. Proteins from various tissue extracts (15 μg) were electrophoresed on SDS-polyacrylamide gels (A) and subjected to immunoblotting with an affinity purified polyclonal antibody, KY-III (B). Asterisk indicates non-specific staining of lens crystallin.

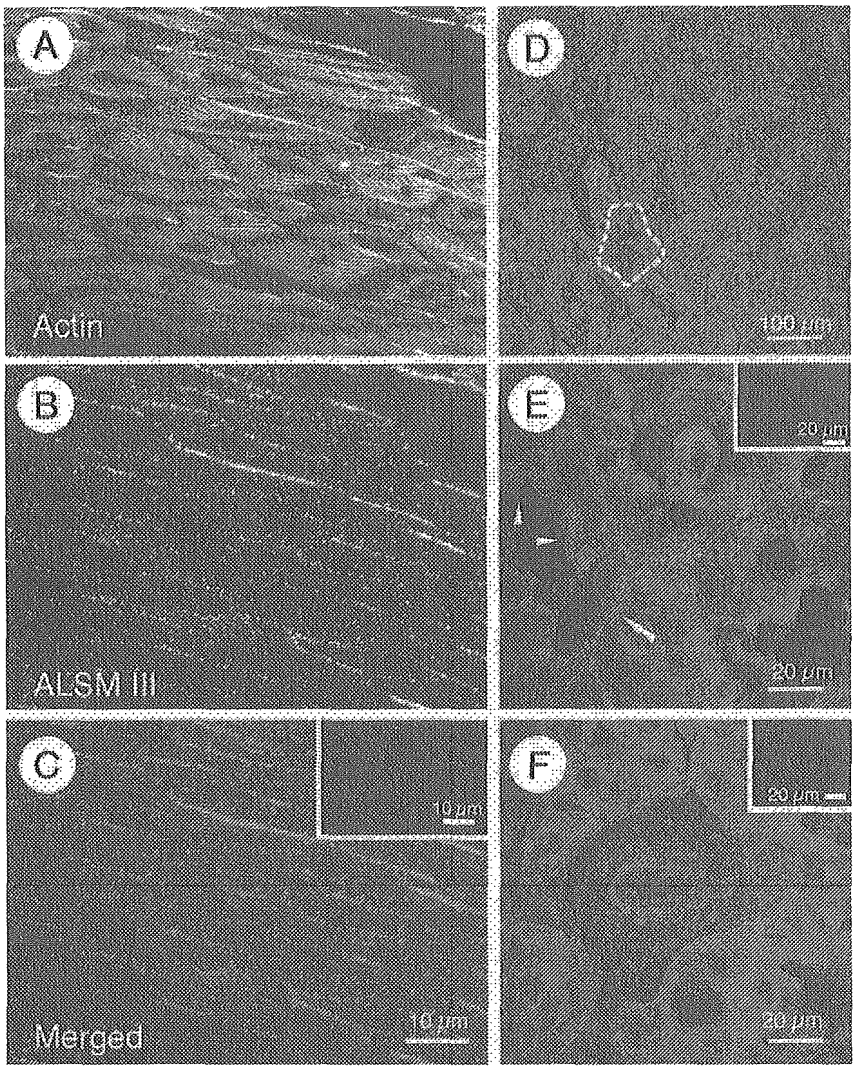

Fig. 9. Immunohistochemical distribution of ALSM III in adult spear squid. Sections of the mantle muscle (A–C) and the liver (D–F) were double stained with anti-actin antibody (red) and KY-III (green). Staining of ALSM III was patchy (B) and distributed extracellularly, unlike the intracellular distribution of actin (A). C, Merged image of (A) and (B). D, Macroscopic view of the liver section with double immunostaining. Squid liver consists of hepatic lobules (dashed-line), like mammal liver. E, High magnification view of boundary area of hepatic lobules. Staining of actin was detected in the boundary area of hepatic lobules (double arrowhead) and periphery of the central vein (arrowheads), whereas staining of ALSM III was detected in hepatic cells. F, High magnification view of interlobular vein. A few layers of actin staining were observed in the vein, whereas staining of ALSM III was weaker in the vein than in hepatic cells. Insert in panel C, E and F shows negative control in the absence of KY-III.

newly hatched squid embryos (stage 28). No immunoreactivity was identified in early stage embryos, which is consistent with in situ hybridization (Fig. 6E and F) and indirect immunofluorescence data (data not shown). Thus, expression of ALSM in squid is unlike that of hatching enzymes. Embryonic expression of astacin family proteins has also been reported in hydra (*Hydra vulgaris*). HMP-1 is secreted from body column endodermal cells at the apical pole, where head regeneration occurs, and it translocates to the tentacles. HMP-1 is involved in cell differentiation or transdifferentiation in tentacle and head regeneration (Yan et al., 1995, 2000b). Both ALSM isoforms were distributed in the fin of the squid embryo; however, ALSM III was confined to the apical region of the fin, suggesting that at least one ALSM isoform contributes to developmental events, as is the case for HMP-1. Distribution of ALSM III in mantle muscle also seems to be developmentally regulated because no detectable immunofluorescence signals were observed in embryonic mantle muscle, whereas apparent singles were detected extracellularly, which is similar to that of ALSM I (Yokozawa et al., 2002).

As shown in Fig. 6, expression of ALSM I mRNA was observed in the liver, and no signal was identified in other tissues. Expression of ALSM III mRNA was also restricted to the liver of embryos (data not shown). Northern blotting and RT-PCR analysis revealed that expression of ALSM mRNAs was restricted to the liver even in the adult squids, suggesting ALSMs are provided only from the liver, beginning at the later stage of embryogenesis and continuing to maturity. However, immunofluorescence study and

immunoblot analysis showed that ALSM III was distributed in a wide variety of tissues, not only in embryos but also in adult squid. These observations indicate that ALSM is a secreted protease produced in the liver that later translocates to several tissues, including muscle and non-muscle tissues. In the present study, we observed ALSM III staining in the iris and in tissue connected to the cornea. In situ hybridization showed no expression of ALSM mRNA in these tissues. Therefore, expression in the iris and in tissue connected to the cornea may be translocated from the liver. We further examined whether ALSM III is present in adult squid eye tissues. However, no signals were detected in these tissues by immunoblot analysis (Fig. 8), or immunofluorescence inspection (data not shown). Thus, distribution of ALSM III in the eyes seems to be developmentally regulated. There are no reports that astacins are involved in eye development or physiological functions of the eye.

In this study, we first showed that expression of ALSM III was higher than that of ALSM I. This result is consistent with the biochemical evidence that in vitro MyHC hydrolysis activity of crude extracts is higher in ALSM III than in ALSM I (Tamori et al., 1999), and purification yields of ALSM III obtained from the same liver extract source as ALSM I are approximately 5-fold (unpublished data), showing that expression of ALSM isoforms is regulated at the transcription level. In summary, our current findings suggest that ALSMs are secreted proteases that are initially expressed at late stages of embryogenesis in the squid liver and then translocate to various muscle and non-muscle tissues. The distribution of ALSM isoforms is differentially regulated, and the isoforms appear to associate with different parts of the tissue. We provide evidence that at least one isoform (ALSM III) contributes to the developmental events of squid. Additional studies are needed to determine the physiologic functions of ALSM isoforms.

Acknowledgements

We are grateful to Dr. Y. Ikeda (Ryukyu University) for providing spear squid embryos and for useful discussions. We thank Drs. I. Iuchi and S. Yasumasu (Sophia University) for valuable comments on this work. This work was supported in part by grants from the Towa Food Research Fund.

References

Baeg, G., Sakurai, Y., Shimazaki, K., 1992. Embryonic stages of *Loligo bleekeri* Keferstein (Mollusca: Cephalopoda). Veliger 35, 234–241.

Bode, W., Gomis-Ruth, F.X., Stocker, W., 1993. Astacins, serralysins, snake venom and matrix metalloproteinases exhibit identical zinc-binding environments (HEXXHXXGXXH and Met-turn) and topologies and should be grouped into a common family, the 'metzincins'. FEBS Lett. 331, 134–140.

Bond, J.S., Beynon, R.J., 1995. The astacin family of metalloendopeptidases. Protein Sci. 4, 1247–1261.

Craig, S.S., Reckelhoff, J.F., Bond, J.S., 1987. Distribution of meprin in kidneys from mice with high- and low-meprin activity. Am. J. Physiol. 253, C535–C540.

Dumermuth, E., Sterchi, E.E., Jiang, W.P., Wolz, R.L., Bond, J.S., Flannery, A.V., Beynon, R.J., 1991. The astacin family of metalloendopeptidases. J. Biol. Chem. 266, 21381–21385.

Fan, T.J., Katagiri, C., 2001. Properties of the hatching enzyme from *Xenopus laevis*. Eur. J. Biochem. 268, 4892–4898.

Henrique, D., Adam, J., Myat, A., Chitnis, A., Lewis, J., Ish-Horowicz, D., 1995. Expression of a Delta homologue in prospective neurons in the chick. Nature 375, 787–790.

Hiroi, J., Maruyama, K., Kawazu, K., Kaneko, T., Ohtani-Kaneko, R., Yasumasu, S., 2004. Structure and developmental expression of hatching enzyme genes of the Japanese eel *Anguilla japonica*: an aspect of the evolution of fish hatching enzyme gene. Dev. Genes Evol. 214, 176–184.

Inohaya, K., Yasumasu, S., Ishimaru, M., Ohyama, A., Iuchi, I., Yamagami, K., 1995. Temporal and spatial patterns of gene expression for the hatching enzyme in the teleost embryo, *Oryzias latipes*. Dev. Biol. 171, 374–385.

Kanzawa, N., Poma, C.P., Takebayashi-Suzuki, K., Diaz, K.G., Layliev, J., Mikawa, T., 2002. Competency of embryonic cardiomyocytes to undergo Purkinje fiber differentiation is regulated by endothelin receptor expression. Development 129, 3185–3194.

Katagiri, C., Maeda, R., Yamashika, C., Mita, K., Sargent, T.D., Yasumasu, S., 1997. Molecular cloning of *Xenopus* hatching enzyme and its specific expression in hatching gland cells. Int. J. Dev. Biol. 41, 19–25.

Laemmli, U.K., 1970. Cleavage of structural proteins during the assembly of the head of bacteriophage T4. Nature 227, 680–685.

Lee, K.S., Yasumasu, S., Nomura, K., Iuchi, I., 1994. HCE, a constituent of the hatching enzymes of *Oryzias latipes* embryos, releases unique proline-rich polypeptides from its natural substrate, the hardened chorion. FEBS Lett. 339, 281–284.

Marques, G., Musacchio, M., Shimell, M.J., Wunnenberg-Stapleton, K., Cho, K.W., O'Connor, M.B., 1997. Production of a DPP activity gradient in the early *Drosophila* embryo through the opposing actions of the SOG and TLD proteins. Cell 91, 417–426.

Mohrlen, F., Hutter, H., Zwilling, R., 2003. The astacin protein family in *Caenorhabditis elegans*. Eur. J. Biochem. 270, 4909–4920.

Okamoto, Y., Otsuka-Fuchino, H., Horiuchi, S., Tamiya, T., Matsumoto, J.J., Tsuchiya, T., 1993. Purification and characterization of two metalloproteinases from squid mantle muscle, myosinase I and myosinase II. Biochim. Biophys. Acta 1161, 97–104.

Piccolo, S., Sasai, Y., Lu, B., De Robertis, E.M., 1996. Dorsoventral patterning in *Xenopus*: inhibition of ventral signals by direct binding of chordin to BMP-4. Cell 86, 589–598.

Sambrook, J., Fritsch, E.F., Maniatis, T., 1989. Molecular Cloning: a Laboratory Manual, 2nd. ed. Cold Spring Harbor Laboratory Press, Cold Spring Harbor, NY.

Sarras Jr, M.P., 1996. BMP-1 and the astacin family of metalloproteinases: a potential link between the extracellular matrix, growth factors and pattern formation. BioEssays 18, 439–442.

Sharrocks, A.D., 1994. A T7 expression vector for producing N- and C-terminal fusion proteins with glutathione S-transferase. Gene 138, 105–108.

Shimell, M.J., Ferguson, E.L., Childs, S.R., O'Connor, M.B., 1991. The *Drosophila* dorsal-ventral patterning gene tolloid is related to human bone morphogenetic protein 1. Cell 67, 469–481.

Steedman, H.F., 1957. A new ribboning embedding medium for histology. Nature 179, 1345.

Tajima, T., Tamori, J., Kanzawa, N., Tamiya, T., Tsuchiya, T., 1998. Distribution of myosinase I and myosinase II in tissues of Coleoidea. Fish. Sci. 64, 808–811.

Takahara, K., Lyons, G.E., Greenspan, D.S., 1994. Bone morphogenetic protein-1 and a mammalian tolloid homologue (mTld) are encoded by

alternatively spliced transcripts which are differentially expressed in some tissues. J. Biol. Chem. 269, 32572–32578.

Takebayashi-Suzuki, K., Yanagisawa, M., Gourdie, R.G., Kanzawa, N., Mikawa, T., 2000. In vivo induction of cardiac Purkinje fiber differentiation by coexpression of preproendothelin-1 and endothelin converting enzyme-1. Development 127, 3523–3532.

Tamori, J., Kanzawa, N., Tajima, T., Tamiya, T., Tsuchiya, T., 1999. Purification and characterization of a novel isoform of myosinase from spear squid liver. J. Biochem. (Tokyo) 126, 969–974.

Titani, K., Torff, H.J., Hormel, S., Kumar, S., Walsh, K.A., Rodl, J., Neurath, H., Zwilling, R., 1987. Amino acid sequence of a unique protease from the crayfish *Astacus fluviatilis*. Biochemistry 26, 222–226.

Vogt, G., Stocker, W., Storch, V., Zwilling, R., 1989. Biosynthesis of Astacus protease, a digestive enzyme from crayfish. Histochemistry 91, 373–381.

Wozney, J.M., Rosen, V., Celeste, A.J., Mitsock, L.M., Whitters, M.J., Kriz, R.W., Hewick, R.M., Wang, E.A., 1988. Novel regulators of bone formation: molecular clones and activities. Science 242, 1528–1534.

Yamaguchi, T., Kido, H., Fukase, M., Fujita, T., Katunuma, N., 1991. A membrane-bound metallo-endopeptidase from rat kidney hydrolyzing parathyroid hormone. Purification and characterization. Eur. J. Biochem. 200, 563–571.

Yan, L., Pollock, G.H., Nagase, H., Sarras Jr., M.P., 1995. A 25.7×10^3 M_r hydra metalloproteinase (HMP1), a member of the astacin family, localizes to the extracellular matrix of *Hydra vulgaris* in a head-specific manner and has a developmental function. Development 121, 1591–1602.

Yan, L., Fei, K., Zhang, J., Dexter, S., Sarras Jr., M.P., 2000a. Identification and characterization of hydra metalloproteinase 2 (HMP2): a meprin-like astacin metalloproteinase that functions in foot morphogenesis. Development 127, 129–141.

Yan, L., Leontovich, A., Fei, K., Sarras Jr., M.P., 2000b. *Hydra* metalloproteinase 1: a secreted astacin metalloproteinase whose apical axis expression is differentially regulated during head regeneration. Dev. Biol. 219, 115–128.

Yasumasu, S., Katow, S., Hamazaki, T.S., Iuchi, I., Yamagami, K., 1992a. Two constituent proteases of a teleostean hatching enzyme: concurrent syntheses and packaging in the same secretory granules in discrete arrangement. Dev. Biol. 149, 349–356.

Yasumasu, S., Yamada, K., Akasaka, K., Mitsunaga, K., Iuchi, I., Shimada, H., Yamagami, K., 1992b. Isolation of cDNAs for LCE and HCE, two constituent proteases of the hatching enzyme of Oryzias latipes, and concurrent expression of their mRNAs during development. Dev. Biol. 153, 250–258.

Yokozawa, Y., Tamai, H., Tatewaki, S., Tajima, T., Tsuchiya, T., Kanzawa, N., 2002. Cloning and biochemical characterization of astacin-like squid metalloprotease. J. Biochem. (Tokyo) 132, 751–758.

New Technology

SNPタイピング法

SNP Typing Methods

徳永　勝士

Key Words
SNP, SNP typing, multifactorial disease, whole genome amplification

■ はじめに

単一遺伝子疾患すなわち遺伝病においては，通常，その原因遺伝子が“まれな変異”であるのに対して，多因子（複合）疾患においては，その感受性遺伝子のほとんどが“SNP（single nucleotide polymorphism，単一塩基多型）などの多型アリル”であると考えられている。疾患感受性遺伝子や薬剤応答性遺伝子の探索研究はもちろん[1]，いわゆるテーラーメイド医療の実現においても，SNPタイピングは必須の要素であり，新しい技術が次々に開発されている[2]。

多数ある方法を，その多型判別原理や測定法に基づいて大別すると以下のようになる。

■ 1．Hybridization法

最も初期から用いられてきたhybridizationを原理とする方法でも，近年，処理能力を一挙に増大させたり，精度を高める技術開発が著しい。現状では，SNP特異的オリゴヌクレオチドプローブをシリコンやガラスなどの基板上に固定するDNAチップ法が主流であり，測定には従来からの蛍光法の他にFRET法や電気化学的方法を用いる方法がある。一方，単純なhybridizationに加えて，SNPの判別に酵素反応を用いる方法として，cleavaseを用いるInvader法や，ligaseとRolling circle DNA amplificationを用いるSniper法などがある。

■ 2．構造の差異を検出する方法

次に，SNP特異的なDNA二本鎖あるいは一本鎖の構造の違いを検出する方法がある。一本鎖DNAが形成する二次構造の違いを検出するSSCP (single strand conformation polymorphism) 法，および標準DNAと検体DNAから形成されるheteroduplexをHPLC (high performance liquid chromatography) で検出する方法が代表的である。

■ 3．特異的伸長反応を利用する方法

また，SNP特異的プライマーによる伸長反応を利用する方法も広く用いられてきた。このために，3’末端がそれぞれのアリルに相補的な二種のプライマーを用意する。伸長産物の測定にはMALDI-TOF/MS (matrix-assisted laser desorption ionization time-of-flight mass spectrometry) を用いる方法のほか，いくつかの方法が開発されている。

■ 4．Sequencing法

さらに，一般の塩基配列決定技術をSNPタイピングに用いることはコスト面や大量検体処理で不利であるが，30塩基程度の配列を簡便に決定するPyrosequencing法などはSNPタイピングにも適している。

■ 5．一分子蛍光検出法

最後に，我々が大規模タイピング用に採用している，SNP特異的プライマー伸長反応と蛍光相関分光法（fluorescent correlation spectroscopy）を組み合わせた一分子蛍光検出法について紹介する。こ

Katsuhi Tokunaga
東京大学医学系研究科人類遺伝学分野：Department of Human Genetics, Graduate School of Medicine, University of Tokyo

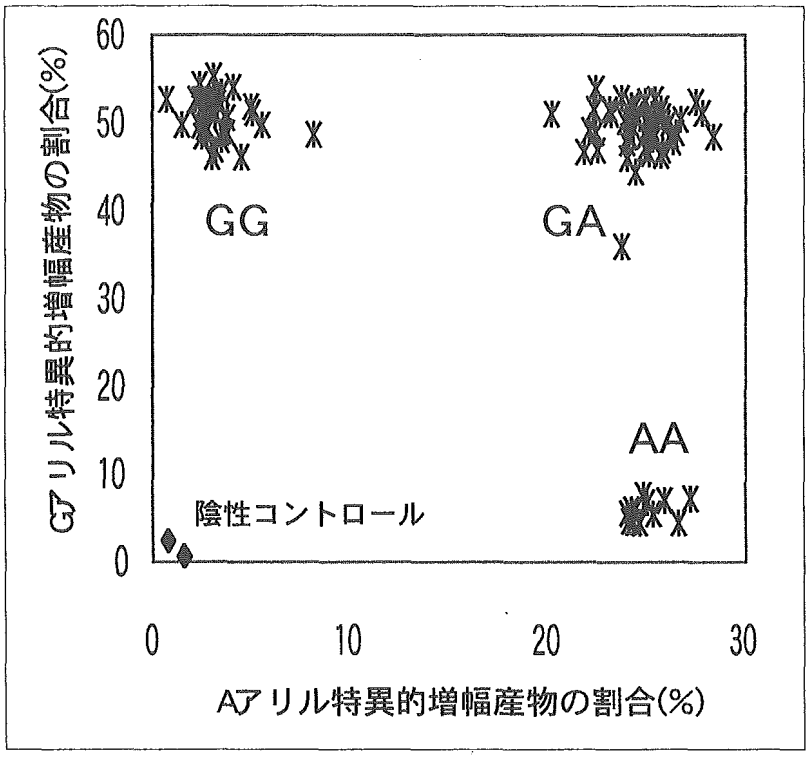

図　Whole genome amplification 処理試料を用いたSNPタイピング例

の方法は1フェムト（10^{-15}）リットルという微小体積を焦点とし，この焦点に出入りする蛍光標識分子に由来する蛍光のゆらぎを，共焦点蛍光顕微鏡下で測定する方法である。この測定法によって蛍光標識された物質の大きさと数を推定することができる。伸長反応が起こらなかった場合には蛍光標識されたプライマーがそのままの大きさ（20 base前後）であるのに対して，伸長反応が起こった場合には大きな産物（100-200 base前後）が標識される。これらの分子の割合を測定することによって，遺伝子型を決定できるというユニークな方法である。この方法の利点はコストが低く，自動化でき，大量検体に適することであろう。最近我々は，一分子蛍光検出法を用いて，whole genome amplification処理後の試料を用いた大量SNPタイピングシステムの確立に成功している[3]。なお，whole genome amplificationは，ある種のランダムプライマーを用いてゲノム全域を断片化して増幅する方法である。我々の経験でも，1回のタイピング分のゲノムDNAから少なくとも100回タイピングできることから，貴重な試料について多数のSNP解析を実施したい場合に有用な方法であるが，個々の試料のqualityのばらつきの影響を受けやすく，多数検体について安定した結果を得ることは決して容易ではない。

文　献

1) 徳永勝士，大橋順：疾患遺伝子の探索．「わかる実験医学シリーズ　ゲノム医科学がわかる」菅野純夫　編：羊土社，p. 48-55, 2001.
2) 馬場真吾，林健志．「わかる実験医学シリーズ　ゲノム医科学がわかる」菅野純夫　編：羊土社，p. 32-39, 2001.
3) Tsuchiya N, Ohashi J and Tokunaga K: Variations in immune response genes and their associations with multifactorial immune disorders. Immunological Reviews 190: 169-181, 2002.

日薬理誌（*Folia Pharmacol. Jpn.*）**123**，55～62（2004）

心不全の重症化機構－その新しい概念－

河田登美枝[1)]，仲澤　幹雄[2)]，豊岡　照彦[3)]

要約：近年，心不全患者は増加しているが，その重症化機構は未だ解明されていない．我々はその機序を先天性と後天性の2つの心不全モデルを用いて検討した．前者として初期から拡張型心筋症を呈するTO-2系ハムスター（TO-2），後者としてイソプレノール（Isp）過量投与ラットを用いた．TO-2ではジストロフィン（Dys）関連タンパク複合体（Dys-Related Protein, DRP）の一つのδ-サルコグリカン（δ-SG）遺伝子が欠損している事を筆者等は同定した．δ-SG遺伝子変異はヒトの拡張型心筋症でも報告されている．DRPの正確な機能は未だ明確ではないが，収縮期の細胞膜の過剰な膨隆を防いで細胞膜の安定性を保つと考えられている．TO-2の心血行動態を経時的に測定し，Dysの組織学的および生化学的変化を観察した．その結果，心筋のDysは加齢と共に細胞膜から細胞質にトランスロケーション（移行）し，細胞膜透過性も増加した．Western blottingの結果，加齢に伴いDysは加水分解され，断片化した．これらの変化は心機能の悪化と一致していた．TO-2に正常配列のδ-SG遺伝子をin vivoで発現させた結果，心機能が改善し，動物の生存率も向上した．δ-SGが発現した細胞では細胞膜の透過性亢進も抑制された．さらにIspを過量投与し急性心不全を起こさせたラットの心筋細胞でもDysの移行と断片化が明瞭に認められ，細胞膜透過性も増加した．一方，δ-SGは変化しなかった．これらの結果は，先天性および後天性心不全とも心不全の進行に伴い心筋細胞膜直下のDysが断片化され，細胞質に移行した結果，細胞膜の安定性は損なわれ，膜透過性が亢進した事が示唆される．以上の事から筆者等は「筋ジストロフィー様の変性が心筋細胞に選択的におこり，その結果心不全が進展する」という作業仮説を提唱する．

キーワード：心不全，ジストロフィン，
ジストロフィン関連タンパク複合体，
細胞膜心筋症

[1)]新潟大学医歯学総合病院・薬剤部
（〒951-8520 新潟市旭町通り1-754）
[2)]新潟大学医学部・保健学科
（〒951-8518 新潟市旭町通り2-746）
[3)]東京大学医学部・器官病態内科
（〒113-0033 東京都文京区本郷7-3-1）

原稿受領日：2003年10月3日，編集委員会依頼総説

1. 背景

心不全は死亡あるいは入院に至る最大の原因である．米国では450万人を占め，日本でも高齢化に伴い患者数は年々増加し，約300万人と推定される．特に重症心不全の予後は不良であり，拡張型心筋症（Dilated Cardiomyopathy, DCM）の場合，心移植の最も高い適応症例である．しかし心移植には社会医学的，臨床的な問題が山積みし，理想的な治療からは程遠い．心不全が重症化する機序は未だ不明である．これを解明し，予防，治療の開発をすることは循環器領域の最大課題の一つである．

重症心不全をきたす疾患としてDCM，広範な心筋梗塞や心筋炎の終末期がある．我々はこれらの疾患が重症化して行く過程を多面的に検討した結果，いずれも疾患末期には心筋細胞内外を結合するジストロフィン関連タンパク複合体（Dystrophin-Related Proteins, DRP）の脱落により，サルコメアの発生張力が細胞外に伝達されず，その結果，重症化する事が示された(1)．

一般に，疾患の病因と治療を確立するためには疾患モデル動物の利用が極めて有用であり，ヒトの肥大型心筋症およびDCMと類似した病態を認める数系の心筋症ハムスターが頻用されている(2)．これらの動物の原因遺伝子は40年近く不明であったが，筆者らはこれらのハムスターでは次に述べるDRPの1つであるδ-sarcoglycan（SG）遺伝子が欠損している事を報告し，そのbreak pointを示した(3)．はじめにDRPについて概説する．

ジストロフィン遺伝子の変異がDuchenneやBecker型の筋ジストロフィー症を起こす事が証明された事がきっかけとなり(4)，ジストロフィンと複合体を形成する多くのタンパク群が発見されている(5,6)．ジストロフィンは細胞膜直下に位置する細長いタンパクで，N端は細胞内の収縮タンパクのアクチンとC端はDRPの中のα-ジスト

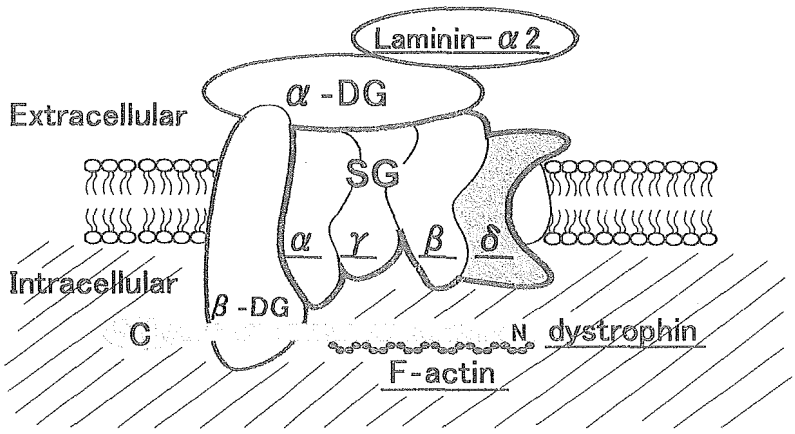

Fig. 1 A scheme of Dystrophin-Related Proteins (DRP). Mutations in DRP, which cause DCM in human cases, are underlined. SG: sarcoglycan, DG: dystroglycan

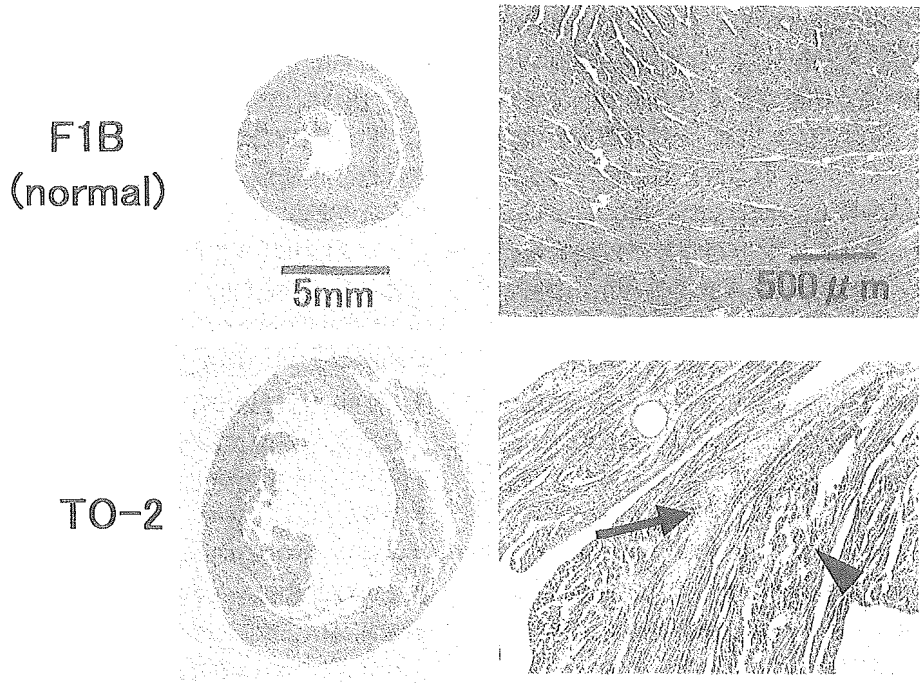

Fig. 2 Microscopic pictures of hamster hearts. The arrows and arrowheads denote the interstitial fibrosis and calcification, respectively.

ログリカン（DG）と結合している．DRPはα-およびβ-DG，α-，β-，γ-およびδ-の4種のSGより構成され，細胞外基質のラミニンα-2と結合している（Fig. 1）．DRPの正確な機能は未だ不明であるが，細胞内の収縮要素と細胞外基質を連結し，収縮期の細胞膜の過剰な膨隆を防いで細胞膜を安定化していると考えられる．

筆者らは先天性の心筋症の原因について心筋細胞膜の構成異常を1992年に指摘した(7)．その後，ヒトDCMにおいてジストロフィン(8)，心筋型アクチン(9)およびデスミン(10)の遺伝子異常も報告された．われわれはδ-SG

の遺伝子欠損を心筋症ハムスターで報告したが(3)，同じδ-SG遺伝子の変異によりDCMを呈したヒトの4家系が報告された(11)．動物で認められた遺伝子変異はヒトでも証明されることが多く，これは人類も他種の動物と同様，分化と環境への順応のために常に変異を起こしてきた証拠である．現在ではδ-SGの他にα-，β-，γ-SG遺伝子と核内タンパクラミンA/Cの変異によるDCMも報告され(12～15)，一連の細胞骨格とDRPが心筋保護に重要な機能を有することが示唆される．

筆者らは初期からDCMを呈するTO-2系ハムスター(TO-2)の心筋細胞に，欠損しているδ-SG遺伝子を強制発現させ，そのレスキューに成功した(16,17)．この研究過程で心不全の重症化機構にDRPが関与することが示唆された．前半はこれらの結果について述べ，後半でラットにイソプロテレノール（以下Isp）を過量投与して急性心不全状態を作製した後天性心不全モデルについて述べる．

2. 先天性心不全モデルによる検討

今回用いた心筋症ハムスターはその遺伝子欠損が自然発症した例であり，人為的に作製したノックアウト動物とは全く異なる．強制的に遺伝子改変したtransgenic動物では多くの代償機構により必ずしも正確に病態を反映しない(18)．自然発症の遺伝子欠損動物に正常遺伝子を安全に発現させる事ができれば積極的な原因治療に繋がり，従来の対症療法的な遺伝子治療とは対照的な治療となる．

この心筋症ハムスターには初期に肥大相を呈し，末期にDCMに至るBIO 14.6系と初期からDCMを呈するTO-2の2種がある．Fig. 2にTO-2の心筋組織像を示す．同系の正常ハムスター（F1B）に比べ，TO-2は心臓が大きく，内腔は顕著に拡大し，左室壁が明らかに薄い．また，瀰漫性に線維化と石灰化がみられる．2002年の本誌に実験技術「生体内心筋に対する遺伝子導入－拡張型心筋症の遺伝子治療」でTO-2を用いた短期（1週間）および中期（10週間）にわたる遺伝子治療の結果は報告した(16,19,20)．遺伝子治療の効果は薬物治療と同様，最終的に動物の生命予後を指標にして判定すべきであると考え，遺伝子導入35週後まで観察した(17)．今回はこの長期実験を中心に解説する．

(1) 実験方法

実験方法の詳細は文献16，17，19-21を参照されたい．δ-SGとレポーター遺伝子のLac Zを同一のCMVプロモーターで駆動した組み換えアデノ随伴ウイルス（recombinant Adeno-Associated Virus, rAAV）ベクターを設計，作製する．rAAVは非分裂細胞にもほぼ生涯にわたり発現が持続し，生体に無害で，現在考えうる最良のウイルスベクターである(22)．既に呼吸器や血液疾患の治療にヒト臨床例で用いられている．rAAVベクターの作製には自治医科大学・遺伝子治療部の小澤敬也教授，卜部　匡先生，および水上浩明先生の協力を頂いた．

5週齢のTO-2を人工呼吸下で開胸し，心尖部心筋層内にレポーター遺伝子のみ（レポーター群），あるいはレポーターとδ-SGの両遺伝子（δ-SG群）を投与した．遺伝子導入35週まで，動物を飼育し，生存率を求めた．この間エコー測定を行なった．実験終了時にカテーテル法にて心血行動態を測定した．さらに正常の細胞膜を透過しないエバンスブルー（EB）を動物に静注し，*in situ*の状態で細胞膜透過性の変化を観察した．心臓を摘出後，心室筋を免疫組織染色用サンプルに供した．

(2) δ-SG遺伝子治療の収縮能，血行動態と予後に及ぼす効果

導入30週後にエコー検査を実施した．レポーター群では収縮末期径（Ds），拡張末期径（Dd）が増加し，左室内径短縮率（FS），左室駆出率（LVEF）が減少し，心室の拡張能と収縮能の減少が顕著だった．レポーター群に比較してδ-SG群ではDs，FSおよびLVEFが有意に改善し，収縮能は向上した(17，Fig. 3)．

40週齢のTO-2では同系の正常動物のF1Bに比べ，左室内圧（F1B対TO-2，125.1±9.6対80±2.8，$P<0.01$）および左室圧最大微分値が低下し（F1B対TO-2，7063±290対4283±97，$P<0.01$），収縮機能は顕著に減少していた．一方，左室圧最小微分値（dP/dt_{min}）が悪化し（F1B対TO-2，−7180±576対−3120±145，$P<0.01$），左室拡張終期圧（LVEDP；F1B対TO-2，1.6±0.9対18.0±1.4，$P<0.01$），中心静脈圧（CVP；F1B対TO-2，−0.6±0.3対9.4±1.4，$P<0.01$）の顕著な上昇が認められ，両心室の拡張機能も極度に低下して鬱血性心不全を呈していた（筆者等，未発表）．この病態はヒトの重症心不全の血行動態所見とよく一致している．レポーター群の遺伝子導入35週後（40週齢）の心血行動態は上記の未処置のTO-2群と同様の値を示した事から，遺伝子導入による影響は認められなかった．一方，責任遺伝子を導入したδ-SG群では悪化していたdP/dt_{min}が有意に改善し，LVEDPおよびCVPは正常化した（Fig. 4A）．この様に両心室の拡張機能および鬱血状態が明らかに改善した．さらに心筋の石灰化と薄くなった左心室壁も遺伝子治療により改善した(17)．

遺伝子導入35週後まで観察した結果，レポーター群では導入4週後から死亡し始め，20週後（25週齢）からは急速に死亡数が増加した．一方δ-SG群ではこの動物の寿命に近い40週齢でも死亡例が無く，生命予後は著明に改善した（Fig. 4B）．これは遺伝子変異による心不全のレスキューに成功した最初の報告である(17)．

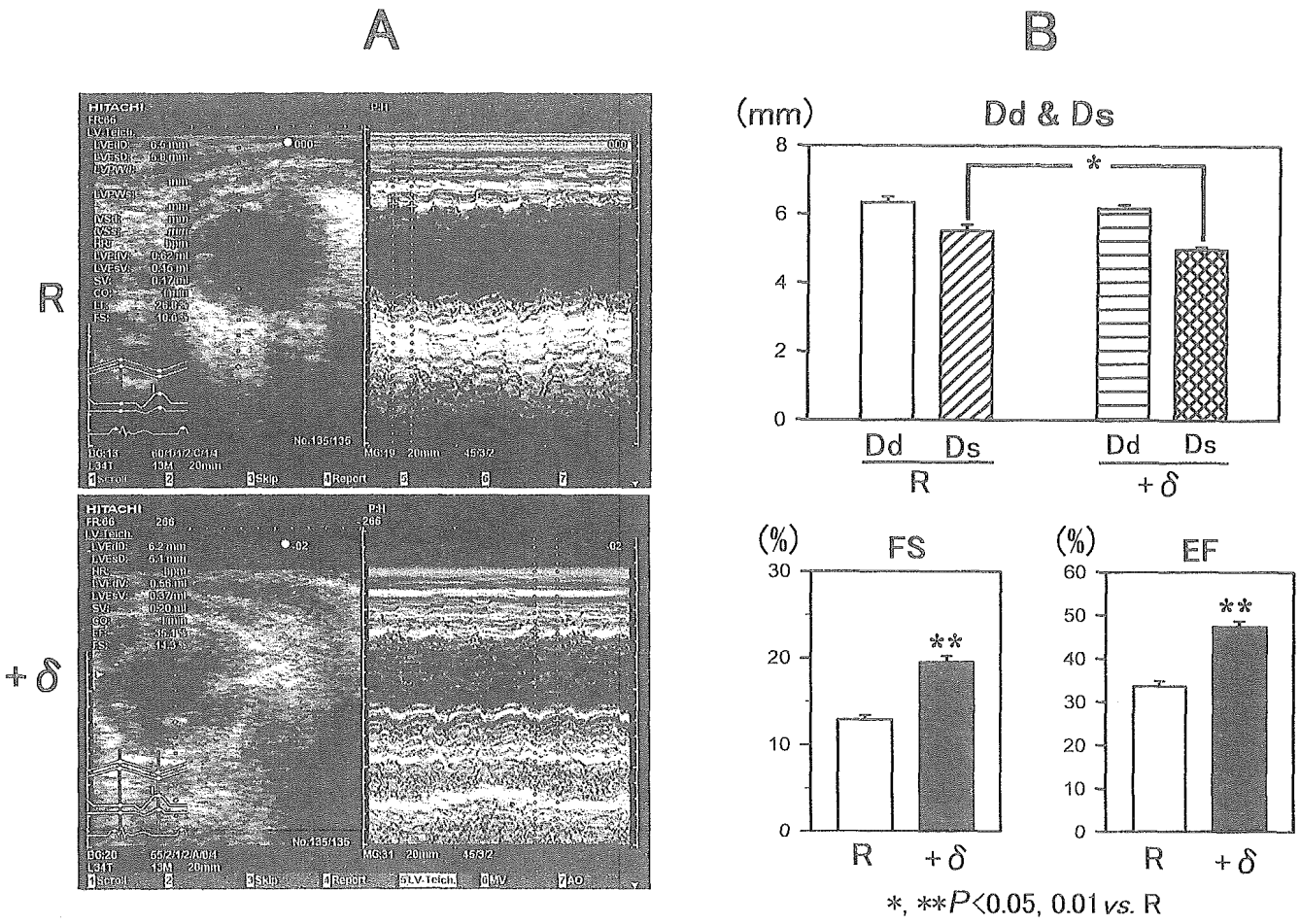

Fig. 3 (A) Short-axes view of the left ventricular cavity by high-frequency (13 MHz) echocardiography and M mode recording in TO-hamsters. (B) Summary of the left ventricular systolic dimension (Ds), the left ventricular diastolic dimension (Dd), fractional shortening (FS), and ejection fraction (EF) in reporter group of animals transfected by the reporter gene alone (R, n=10) or δ group cotransfected by the reporter gene plus normal δ-SG genes (+δ, n=10). In the δ group, the enlarged Ds, reduced FS and decreased EF were improved, compared with the reporter group (Ref 17).

(3) 細胞膜透過性と心不全

実験終了時にEBを静注後，心臓を摘出し *in situ* で細胞膜透過性を検討した．細胞膜が正常ならば，EBは膜を通過しない．一方，細胞膜が脆弱になり，膜透過性が増すとEBは細胞内に流入し，赤い蛍光を発する．FITCでラベルしたδ-SG抗体とEBを同一視野で二重蛍光観察することにより，タンパク発現と膜透過性を同時に検出する事が可能である．δ-SG群では心筋細胞にδ-SGが発現し，その細胞ではEBは認められなかったが，レポーター群ではδ-SGは発現せず，一部の細胞にはEBが流入し，膜透過性が増大していた．遺伝子が導入された全細胞数に対するEB-陽性細胞の割合はレポーター群に比べ，遺伝子治療群では約1/5に減少し，細胞膜透過性の増大が著明に抑制された．これらの結果の詳細は文献17を参照されたい．以上の結果からDRPの変異や崩壊により筋細胞膜が脆弱化して，心不全を来たすと考えられる．δ-SG遺伝子補充治療は心筋細胞膜機能を直接保護する事により心不全の悪化と生命予後を改善する事が示された．

(4) ジストロフィンの崩壊と心不全

TO-2は先天的なδ-SG遺伝子欠損にもかかわらず，幼若期には心不全症状は認められず，その成長に伴って症状が悪化していくが(23, 24，筆者等，未発表)，その理由は

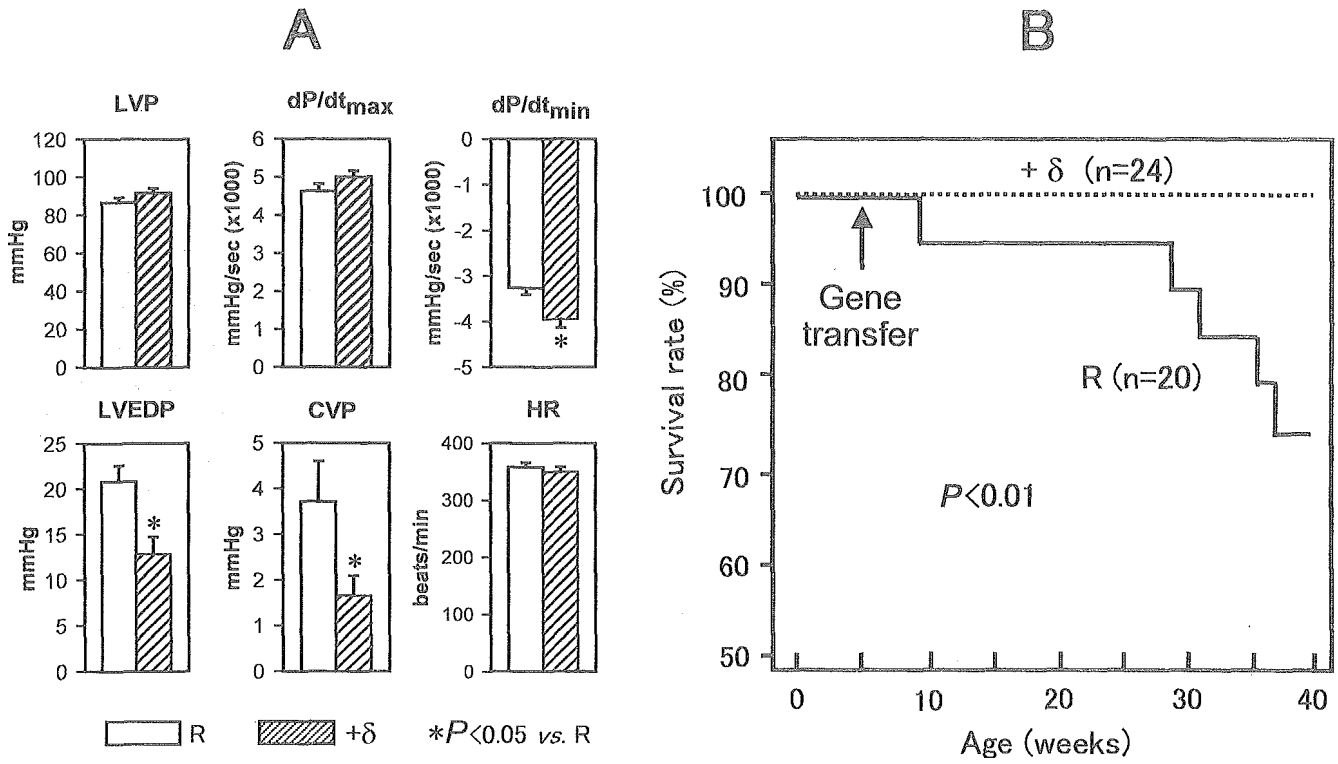

Fig. 4 (A) Improvement of hemodynamic indices at 35 weeks after the gene therapy with recombinant adeno-associated virus vector (rAAV). R: reporter group transfected by the reporter gene alone (n=12); +δ: δ group cotranfected by the reporter gene plus normal δ-SG genes (n=18); LVP: left ventricular pressure; dP/dt_{max}: maximum derivative of LVP; dP/dt_{min}: minimum derivative of LVP; LVEDP: the left ventricular end-diastolic pressure, CVP; central venous pressure, HR; heart rate. (B) Mortality of TO-2 by Kaplan-Meier analysis after gene therapy. In the reporter group (R), 5 animals died during the 35 weeks. In contrast, all animals in the δ-SG gene transfected group (+δ) survived (Ref 17).

未だ解明されていない．我々はδ-SG遺伝子の欠損によりDRPと連結しているジストロフィンが徐々に崩壊していく，すなわち筋ジストロフィー様の病変が心筋選択的に発生した結果，心不全が進展すると考えた．この仮説を検証するために，TO-2の心血行動態を経時的に測定した．次に心筋細胞を摘出し，ジストロフィンの組織学的および生化学的な変化を同時に観察した．

現在，投稿中のため詳細な結果は示さないが，以下のことが判明した．心血行動態の測定の結果，F1Bでは週齢に伴う顕著な変化はなかったが，TO-2では15週からうっ血性心不全症状を呈し，特に25週から40週の間で顕著に悪化した．TO-2では加齢に伴い心室筋細胞のジストロフィンが分子量の小さいバンドに断片化し，細胞膜から細胞質へトランスロケーション（移行）した．EBの蛍光がトランスロケーションした細胞内に認められ，細胞膜透過性が上昇したことが示唆された．この変化は心不全の重症化と一致していた．さらに遺伝子治療を行いδ-SGが発現した心筋細胞では，ジストロフィンのトランスロケーションと細胞膜透過性亢進が抑制された．従来心筋症ハムスターにおいてδ-SG遺伝子の欠損がDCMの原因であり，ジストロフィンの崩壊は無いと考えられてきたが，これらの結果は心筋症ハムスターにでも心不全が重症化するに伴い，ジストロフィンが心筋細胞膜より細胞質へ遊離し，断片化され，細胞膜が脆弱になる事が示された．

3. 後天性心不全モデル

ラットにβ刺激薬のIspを過量投与すると急性心不全が起こる事はよく知られている．ヒトにおいても心不全の進展に伴い血漿中のカテコールアミン量は著明に上昇する．βアゴニストの投与は心不全患者の心機能と予後を悪化す

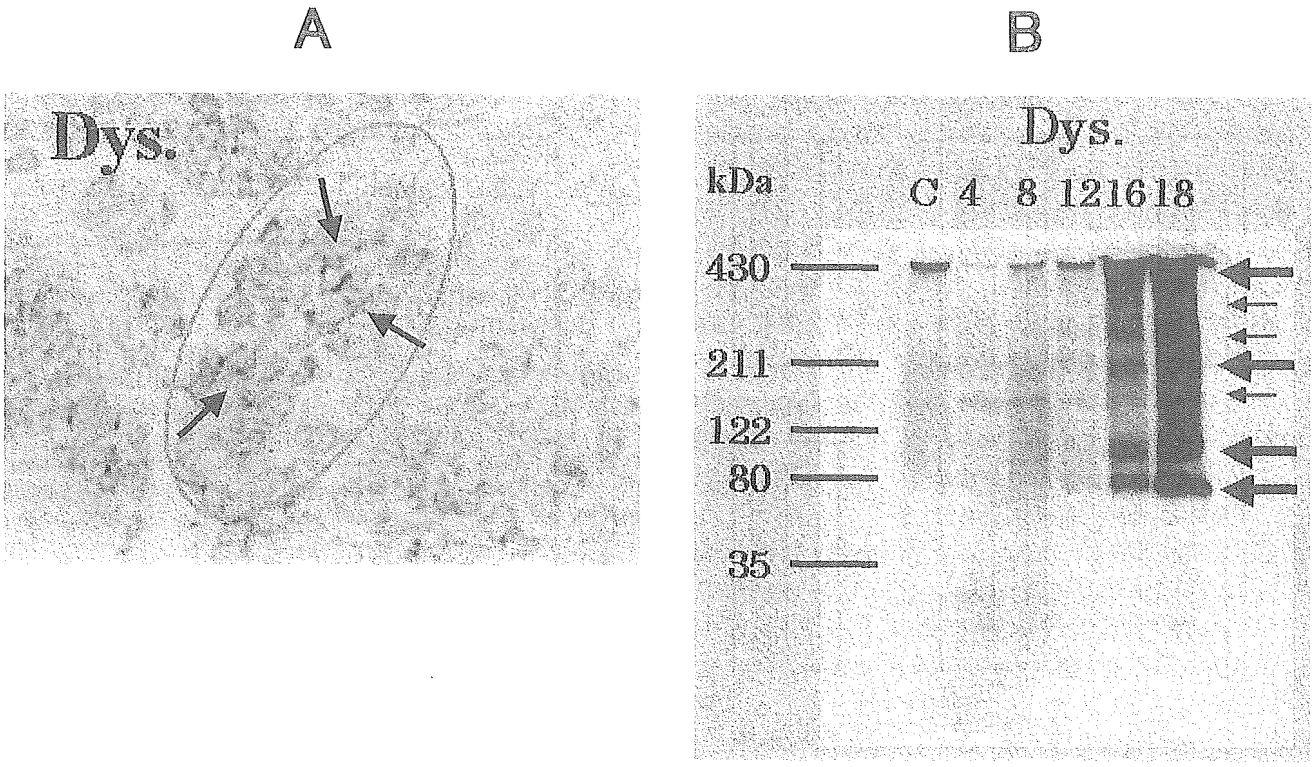

Fig. 5 Time-dependent fragmentation of dystrophin (Dys.) after the administration of isoproterenol (Isp) at high dose. Dys was disrupted by Isp, translocated, and fragmented (Ref 25).

る．一方，カルベジロールに代表されるβ遮断薬は死亡率と疾病率を改善する．これらの事から心不全の進展に交感神経系の刺激が関与すると考えられている．しかし，その作用機序は未だ解明されていない．我々はIsp過量投与心不全ラットにおいてジストロフィンの組織学的および生化学的検討を行った(25)．

Isp投与後，左心室の心筋障害は経時的に進展した．心筋細胞をジストロフィンの特異抗体で染色すると，ジストロフィンは細胞膜に均一には染色されず，一部の細胞では細胞膜から細胞質にトランスロケーションした（Fig. 5A）．Western blottingの結果，正常心筋ではジストロフィンの分解は認められなかったが，Isp投与後の時間経過に伴い，分子量の小さいバンドに断片化された（Fig. 5B）．図は示さないが，この時，細胞膜透過性も増加していた．一方，δ-SGは細胞膜に局在し，Western blottingにおいてもIsp投与群は対照群と同様の単一バンドを示し，全く分解されなかった（筆者等，未発表）．

又，心筋梗塞後の心不全モデルでも残存心筋中のα-SGとジストロフィンが崩壊することも今年度に報告した(26)．したがって，先天的なDCMの結果と同様に後天的な心不全もジストロフィンの分解により細胞膜の透過性が高まり，膜が脆弱になった結果，心筋が傷害されたと考えられる．

4. 考察

われわれはDCMハムスターに欠損していたδ-SG遺伝子を導入する事により，小型動物レベルではあるが，世界に先駆けて先天性DCMの遺伝子治療の開発に成功した(16,17)．δ-SGはDRPを構成するタンパクの1つで，DRPは収縮期の細胞膜の過剰な膨隆を防ぎ，細胞膜を安定化すると考えられている．心筋は収縮・弛緩を生涯恒常的に繰り返す必要から，その細胞膜は骨格筋以上に強靭さが要求される．筆者等の研究では先天性DCMおよび後天性心不全とも，心不全の進行にともない心筋細胞膜直下にあるジストロフィンが断片化し，細胞質にトランスロケーションし，細胞膜の透過性が高まることを示した．また最近，我々はTO-2心筋細胞での免疫電顕の結果，細胞膜ではδ-SGは完全に欠損し，ジストロフィンは部分的に欠落する事を報告した(27)．以上から各種の先天性，および後天性の原因によりDRPが崩壊し，筋ジストロフィー様の病態が心筋細胞に選択的におこり，その結果心不全が進展

するという作業仮説を提唱する．

Bardorff等はprotease 2A geneを持っているenterovirus（Coxsackie B3）をマウスに感染させ，心筋症類似の心不全を起こさせた．この時に心筋細胞ではジストロフィンが分断された(28)．また，Towbin等はヒトのDCMあるいは虚血性による心不全末期の患者の心筋細胞ではN末端でジストロフィンが崩壊することを示した(29)．この現象は左室補助装置（LV assistant device）で改善するため，ジストロフィンの崩壊は可逆的である事が示唆される．筆者等も拡張型心筋症ハムスターの心筋細胞にrAAVを用いて責任遺伝子を発現させた結果，ジストロフィンのトランスロケーションと細胞膜の透過性は改善し，最終的に動物はレスキューされることを示した(筆者等，未発表)．これらの事実はジストロフィンの崩壊により心不全が重症化するという我々の仮説を支持する．

前述のようにDRPの変異によるヒトDCMは報告されている(11)．先天的な遺伝子変異によるDCMの症例はヒトゲノム計画が成功した現段階では解析法の進歩により今後更に増加すると思われる．原因遺伝子が解明されれば，遺伝子治療によるレスキューの可能性は増してくる．また原因遺伝子が不明な場合でも，ジストロフィンの崩壊を抑制する新たな治療法の開発が期待される．

謝辞：本研究を推進する上で終始御支援を頂いた国立生理学研究所・江橋節郎名誉所長，国立循環器病センター研究所・真崎知生名誉所長，独立行政法人・産業総合研究所(旧工業技術院)・年齢軸研究センター・倉地幸徳センター長および，資金面で研究助成を頂いた文部科学省，厚生労働省，学術振興会，三菱財団，車輌財団に深謝申し上げる．

文　献

1) Toyo-oka T, Kawada T, Xi H, et al. Gene therapy prevents disruption of dystrophin-related proteins in a model of hereditary dilated cardiomyopathies in hamster. Heart Lung Circ. 2002;11:174-181.
2) Homburger F, Baker JR, Nixon CW, et al. Primary, generalized polymyopathy and cardiac necrosis in an inbred line of Syrian hamsters. Med Exp. 1962; 6:339-345.
3) Sakamoto A, Ono K, Abe M. et al. Both hypertrophic and dilated cardiomyopathies are caused by mutation of the same gene, δ-sarcoglycan, in hamster: an animal model of disrupted dystrophin-associated glycoprotein complex. Proc Natl Acad Sci USA. 1997;94:13873-13878.
4) Hoffman EP, Brown RJ, Kunkel LM. Dystrophin: the protein product of the Duchenne muscular dystrophy locus. Cell. 1987;51:919-928.
5) Cox GF, Kunkel LM. Dystrophies and heart disease. Curr Opin Cardiol. 1997;12:329-343.
6) Seidman JG, Seidman C. The genetic basis for cardiomyopathy: from mutation identification to mechanistic paradigms. Cell. 2001;104:557-567.
7) Toyo-oka T, Nagayama K, Suzuki J. et al. Noninvasive assessment of cardiomyopathy development with simultaneous measurement of topical ^{1}H- and ^{31}P-magnetic resonance spectroscopy. Circulation. 1992;86:295-301.
8) Muntoni F, Cau M, Ganau A, et al. Brief report: deletion of the dystrophin muscle-promoter region associated with X-linked dilated cardiomyopathy. N Engl J Med. 1993;329:921-925.
9) Olson TM, Michels VV, Thibodeau SN, et al. Actin mutations in dilated cardiomyopathy, a heritable form of heart failure. Science. 1998;280:750-752.
10) Li D, Tapscoft T, Gonzalez O, et al. Desmin mutation responsible for idiopathic dilated cardiomyopathy. Circulation. 1999;100:461-464.
11) Tsubata S, Bowles KR, Vatta M, et al. Mutations in the human δ-sarcoglycan gene in familial and sporadic dilated cardiomyopathy. J Clin Invest. 2000;106:655-662.
12) Fadic R, Sunada Y, Waclawik AJ, et al. Brief report: deficiency of a dystrophin-associated glycoprotein (adhalin) in a patient with muscular dystrophy and cardiomyopathy. N Engl J Med. 1996;334: 362-366.
13) Barresi R, Di Blasi C, Negri T, et al. Disruption of heart sarcoglycan complex and severe cardiomyopathy caused by a sarcoglycan mutations. J Med Genet. 2000;37:102-107.
14) Politano L, Nigro V, Passamano L, et al. Evaluation of cardiac and respiratory involvement in sarcoglycanopathyies. Neuromuscul Disord. 2001; 11:178-185.
15) Fatkin D, MacRae C, Sasaki T, et al. Missense mutations in the rod domain of the lamin A/C gene as causes of dilated cardiomyopathy and conduction-system disease. N Engl J Med. 1999;341:1759-1762.
16) Kawada T, Sakamoto A, Nakazawa M, et al. Morphological and physiological restorations of hereditary form of dilated cardiomyopathy by somatic gene therapy. Biochem Biophys Res Commun. 2001;284:431-435.
17) Kawada T, Nakazawa M, Nakauchi S, et al. Rescue of hereditary form of dilated cardiomyopathy by rAAV-mediated somatic gene therapy. Proc Natl Acad Sci USA. 2002;99:901-906.
18) Huang WY, Aramburu J, Douglas PS, et al. Transgenic expression of green fluorescence protein can cause dilated cardiomyopathy. Nat Med. 2000;6:482-483.
19) 河田登美枝，仲澤幹雄，豊岡照彦．生体内心筋に対する遺伝子導入－拡張型心筋症の遺伝子治療．日薬理誌. 2002;119:37-44.
20) Kawada T, Nakatsuru Y, Sakamoto A, et al. Strain- and age-dependent loss of sarcoglycan complex in cardiomyopathic hamster hearts and its re-expression by δ-sarcoglycan gene transfer in vivo. FEBS Lett. 1999;458:405-408.
21) Kawada T, Shin WS, Nakatsuru Y, et al. Precise identification of gene-products in hearts after *in vivo* gene transfection, using Sendai virus-coated